

Synthesis and Electrical Characterisation of the Apatite-type Oxide Ion Conductors $\text{Nd}_{9.33+x}\text{Si}_{6-y}\text{Ga}_y\text{O}_{26+z}$

J.R. Tolchard, J.E.H. Sansom, M.S. Islam and P.R. Slater*

Chemistry, SBMS, University of Surrey, Guildford, Surrey, GU2 7XH, UK

*Corresponding author:

e-mail: p.slater@surrey.ac.uk Tel. +44 (0)1483 686847, Fax +44 (0)1483 686851

Abstract. Apatite-type oxides have been attracting interest as a new class of oxide ion conductors. In this paper we examine the effect of Ga doping on the conductivity of the apatite silicate system, $\text{Nd}_{9.33+x}\text{Si}_6\text{O}_{26+3x/2}$ and compare the results to those reported for similar doping studies in $\text{La}_{9.33+x}\text{Si}_6\text{O}_{26+3x/2}$. The highest conductivities are observed for samples containing oxygen excess, which is in agreement with previous reports that interstitial oxide ions are important for high oxide ion conduction in these materials. For oxygen stoichiometric materials, i.e. $\text{Nd}_{9.33+x/3}\text{Si}_{6-x}\text{Ga}_x\text{O}_{26}$, the Ga doping results in a significant increase in activation energy and a consequent lowering of the low temperature conductivity. This is contrary to results previously reported for the La containing analogues, which showed an enhancement of conductivity on Ga doping up to $x = 1.5$. Possible explanations for the differences between the two systems are discussed.

1. Introduction

Research into solid state oxide ion conductors is attracting considerable interest due to their potential use in a range of technological applications, such as solid oxide fuel cells, oxygen sensors and separation membranes. In this respect interest has traditionally focused on materials with the fluorite, perovskite or related structures, although recently other structure types have been attracting attention. One such example is the apatite-structure after the initial reports of Nakayama et al. of high oxide ion conductivity in rare earth silicates with this structure [1-3]. These oxide ion conducting apatites, $(\text{Ln})_{10-x}(\text{Si}/\text{Ge})_6\text{O}_{26+y}$ (Ln = rare earth), represent a new class of oxide ion conductor, and have been attracting significant interest [1-24]. Their crystal structure is shown in figure 1; it consists of isolated Si/GeO₄ tetrahedra with the rare earth cations located in 7 coordinate and 9 coordinate cavity sites. The extra oxide ions occupy channels running through the structure, and it is these oxide ion channels that are responsible for the high oxide ion conduction. These phases have great scope

for modifications through doping studies, with a wide range of dopants reported, e.g. rare earth site: alkali metals, alkaline earth metals, Bi, Mn, Co; Si/Ge site: B, Al, Ga, Fe, Co, Mn, P [9,11,14,15,18-20,22-24].

Since these systems are quite complex structurally it is important to be able to rationalise the relationship between structure and properties, and this has been a key aim of our research. Our early work showed that fully stoichiometric systems, e.g. $\text{La}_8\text{Sr}_2\text{Si}_6\text{O}_{26}$, had much lower conductivities and higher activation energies than systems that contained either cation vacancies, e.g. $\text{La}_{9.33}\text{Si}_6\text{O}_{26}$, or oxygen excess, e.g. $\text{La}_9\text{SrSi}_6\text{O}_{26.5}$ [13]. Neutron diffraction experiments on the compounds $\text{La}_{9.33}\text{Si}_6\text{O}_{26}$ and $\text{La}_8\text{Sr}_2\text{Si}_6\text{O}_{26}$ showed that these materials have significant complexities in their structures, particularly within the channel oxygen sites [13], with the former sample showing significant disorder within the channels, in the form of interstitial oxygens. The importance of interstitial oxygens was further supported by our computer modelling studies on $\text{La}_{9.33}\text{Si}_6\text{O}_{26}$ and $\text{La}_8\text{Sr}_2\text{Si}_6\text{O}_{26}$, which suggested that oxide ion conduction

proceeded via an interstitial mechanism in $\text{La}_{9.33}\text{Si}_6\text{O}_{26}$, while for $\text{La}_8\text{Sr}_2\text{Si}_6\text{O}_{26}$ the mechanism involved vacancy migration [16, 17]. The modelling studies predicted the presence of an energetically favourable oxygen interstitial position located at the periphery of the channels. Furthermore, a complicated interstitial migration mechanism, which was strongly dependant on the ability of the silicate substructure to relax towards the La sites that contain the cation vacancies, was also predicted. Further support for the presence of such interstitial oxide ions has come from recent structural studies of oxygen excess systems, $\text{La}_{9.33+x}(\text{Si}/\text{Ge})_6\text{O}_{26+3x/2}$ [21], and Mössbauer studies of Fe doped samples [22,23].

In a recent paper we compared the conductivities of a range of oxygen stoichiometric lanthanum silicate apatite samples with dopants on either the La site (Mg, Ca, Sr, Ba) or the Si site (B, Ga) [24]. This study showed that the latter doping strategy gave samples with higher conductivity suggesting the importance of the tetrahedral sites to the conduction process as predicted by modelling studies. In this paper we extend this investigation to look at the effect of reducing the size of the rare earth in the Ga doped samples. To this end a series of Ga doped $\text{Nd}_{9.33+x}\text{Si}_6\text{O}_{26+3x/2}$ phases have been prepared and their conductivities determined. The results are compared to those obtained for similar doping in the La containing analogues, $\text{La}_{9.33+x}\text{Si}_6\text{O}_{26+3x/2}$. This represents a good comparison since the conductivity of undoped $\text{Nd}_{9.33+x}\text{Si}_6\text{O}_{26+3x/2}$ is similar to that of $\text{La}_{9.33+x}\text{Si}_6\text{O}_{26+3x/2}$ [1-3, 12, 13, 19], and so any significant differences in the doped samples can be assigned to the influence of the Ga dopant.

2. Experimental Description

High purity Nd_2O_3 , SiO_2 and Ga_2O_3 were used to prepare a range of $\text{Nd}_{9.33+x}\text{Si}_6\text{O}_{26+3x/2}$ samples doped with Ga. The starting materials were ground in the appropriate ratios and heated to 1300 °C for 16 hours. The samples were then reground and reheated to 1350 °C for a further 16 hours. Phase purity was examined using powder X-ray diffraction (Seifert 3003TT X-ray diffractometer).

Conductivities were determined using a.c. impedance measurements (Solartron 1260 impedance analyser). Dense pellets (1.6 cm diameter) of each sample were prepared by pressing at 6000 kg cm⁻² and sintering at 1500-1600 °C for 2 hours. Both sides of the pellet were coated with Pt paste to act as electrical contact for the measurements.

Table 1. Cell parameters (hexagonal cell): Neodymium silicate apatites doped with Ga.

Sample	a (Å)	c (Å)
$\text{Nd}_{9.33}\text{Si}_6\text{O}_{26}$	9.564(3)	7.025(3)
$\text{Nd}_{9.67}\text{Si}_6\text{O}_{26.5}$	9.569(3)	7.028(2)
$\text{Nd}_{9.5}\text{Si}_{5.5}\text{Ga}_{0.5}\text{O}_{26}$	9.576(4)	7.042(3)
$\text{Nd}_{9.67}\text{Si}_5\text{GaO}_{26}$	9.597(3)	7.059(3)
$\text{Nd}_{9.83}\text{Si}_{4.5}\text{Ga}_{1.5}\text{O}_{26}$	9.622(5)	7.072(4)
$\text{Nd}_{1.0}\text{Si}_4\text{Ga}_2\text{O}_{26}$	9.636(4)	7.085(4)
$\text{Nd}_{1.0}\text{Si}_3\text{GaO}_{26.5}$	9.592(4)	7.065(3)

Table 2. Conductivity data: Neodymium silicate apatites doped with Ga.

Sample	$\sigma_{500^\circ\text{C}}$ /Scm ⁻¹	$\sigma_{800^\circ\text{C}}$ /Scm ⁻¹	Ea/eV (low/high temp.)
$\text{Nd}_{9.33}\text{Si}_6\text{O}_{26}$	1.01×10^{-4}	1.30×10^{-3}	0.72
$\text{Nd}_{9.67}\text{Si}_6\text{O}_{26.5}$	1.56×10^{-3}	9.84×10^{-3}	0.66/0.49
$\text{Nd}_{9.5}\text{Si}_{5.5}\text{Ga}_{0.5}\text{O}_{26}$	7.41×10^{-5}	1.24×10^{-3}	0.75
$\text{Nd}_{9.67}\text{Si}_5\text{GaO}_{26}$	1.63×10^{-5}	8.55×10^{-4}	1.04
$\text{Nd}_{9.83}\text{Si}_{4.5}\text{Ga}_{1.5}\text{O}_{26}$	1.79×10^{-5}	1.05×10^{-3}	1.04
$\text{Nd}_{1.0}\text{Si}_4\text{Ga}_2\text{O}_{26}$	4.22×10^{-7}	5.31×10^{-5}	1.24
$\text{Nd}_{1.0}\text{Si}_3\text{GaO}_{26.5}$	1.31×10^{-4}	4.04×10^{-3}	0.92

3. Results and Discussion

A range of samples were successfully prepared to include samples stoichiometric in oxygen, i.e. $\text{Nd}_{9.33+x/3}\text{Si}_6\text{O}_{26}$, as well as samples containing oxygen excess, i.e. $\text{Nd}_{9.67+x/3}\text{Si}_6\text{Ga}_x\text{O}_{26.5}$. Cell parameters for these samples are given in Table 1. In agreement with the larger size of Ga^{3+} given in Table 1. In agreement with the larger size of Ga^{3+} versus Si^{4+} , an increase in the cell parameters was observed with increasing Ga content.

Conductivity data are given in Table 2. From the data it can be seen that the highest conductivities were observed for samples containing cation vacancies or oxygen excess, with the latter giving the highest conductivities. This is consistent with previous reports on the conductivities of apatite systems and supports the importance of interstitial oxide ions. In terms of the undoped samples, $\text{Nd}_{9.33+x}\text{Si}_6\text{O}_{26+3x/2}$, similar conductivity

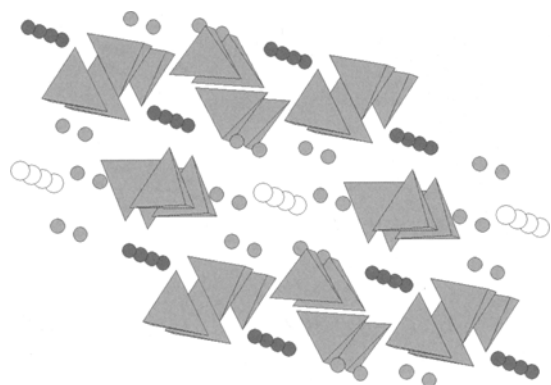


Fig. 1. The apatite, $\text{Ln}_{10-x}(\text{Si/Ge})_6\text{O}_{26+y}$, structure. Dark spheres = Ln, Light spheres = O, tetrahedra = Si/GeO₄.

data were observed to previous reports and the La analogues, $\text{La}_{9.33+x}\text{Si}_6\text{O}_{26+3x/2}$ [1-2,12,13,19].

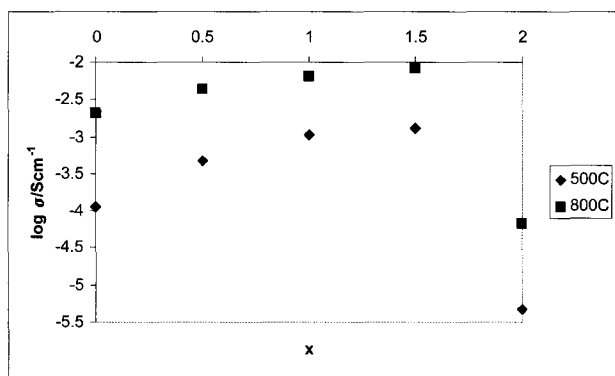


Fig. 2(a). Plot of $\log \sigma_{500^\circ\text{C}}$ and $\log \sigma_{800^\circ\text{C}}$ versus Ga content (x) for $\text{La}_{9.33+x/3}\text{Si}_{6-x}\text{Ga}_x\text{O}_{26}$.

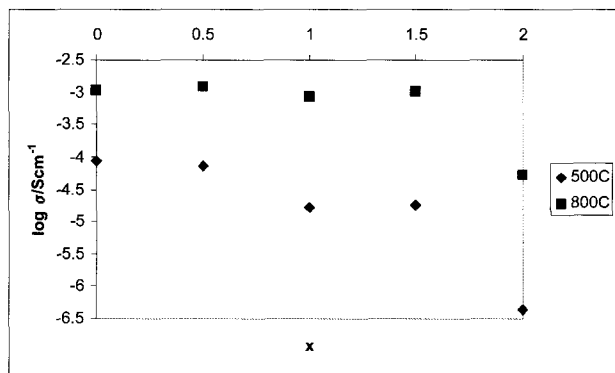


Fig. 2(b). Plot of $\log \sigma_{500^\circ\text{C}}$ and $\log \sigma_{800^\circ\text{C}}$ versus Ga content (x) for $\text{Nd}_{9.33+x/3}\text{Si}_{6-x}\text{Ga}_x\text{O}_{26}$.

A comparison of the data for the Ga doped $\text{Nd}_{9.33+x}\text{Si}_6\text{O}_{26+3x/2}$ samples with previous literature data for Ga doped $\text{La}_{9.33+x}\text{Si}_6\text{O}_{26+3x/2}$ [20,24], showed some significant differences, which was particularly noticeable for samples stoichiometric in oxygen, i.e. $\text{Ln}_{9.33+x/3}\text{Si}_6\text{Ga}_x\text{O}_{26}$ (Ln=Nd, La). For such samples with Ln=La, previous studies have shown that Ga doping leads to an initial increase in conductivity on increasing substitution (up to $x = 1.5$) and correspondingly reducing the number of La cation vacancies. A decrease in conductivity is then observed as the Ga doping level is increased further, and the fully (cation and anion) stoichiometric ($x = 2$) phase is approached (Fig. 2a) [20,24]. These results are also supported by reported studies on Al and B substitutions on the Si site [14, 24]. This increase in conductivity in the case of Ga (and Al, B) substitution on the Si site is interesting, and it relevant to note that our previous computer modelling studies have predicted that the tetrahedral framework plays a key role in the conduction process, aiding the migration of the interstitial oxide ions down the channels [16, 17]. This would then suggest that the presence of lower valent cations on this site is beneficial to the conduction for samples stoichiometric in oxygen.

In the case of the Nd containing samples, however, Ga doping produced a reduction in the conductivity at low temperatures accompanied by a higher activation energy (Table 2, Figs. 2b and 3). As the temperature was raised, the conductivity approaches that of the undoped sample, as a result of the higher activation energy for the Ga doped samples.

This significantly different effect of Ga doping in $\text{Nd}_{9.33}\text{Si}_6\text{O}_{26}$ to $\text{La}_{9.33}\text{Si}_6\text{O}_{26}$ is interesting and requires

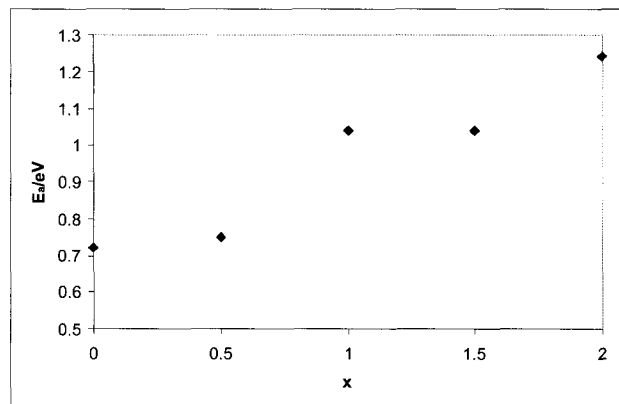


Fig. 3. Plot of E_a versus Ga content (x) for $\text{Nd}_{9.33+x/3}\text{Si}_{6-x}\text{Ga}_x\text{O}_{26}$.

further discussion. The key effect seems to be a significant increase in the activation energy for the former (Table 2, Fig. 3). This increased activation energy could be due to two possibilities.

1. A reduction in the concentration of oxygen interstitials, so that the higher activation energy is due to a combination of the energy to create these oxygen interstitials and the energy for their migration.
2. The interstitial oxygen ions are still present, but the Ga doping either influences the conduction pathway resulting in a higher migration energy or causes "trapping" of the interstitial ions, so that an additional contribution to the activation energy is required to free them.

As the higher activation energy is also observed for the sample, $\text{Nd}_{10}\text{Si}_5\text{GaO}_{26.5}$, which contains oxygen excess, this would suggest that the 2nd explanation is the most likely.

Of relevance to this discussion are our recent modelling studies on the incorporation of dopants into these apatite-type oxides. This work has so far concentrated on the $\text{La}_{9.33}\text{Si}_6\text{O}_{26}$ system, and studies have examined both the favourability of a dopant for a particular site, as well as investigating the local distortions caused by the incorporation of the dopant [25]. The modelling studies of Ga doping in $\text{La}_{9.33}\text{Si}_6\text{O}_{26}$ have shown that although the tetrahedral unit is seen to expand significantly on incorporation of the larger Ga in place of Si, the accommodation of this expansion in the structure as a whole is quite complex. Overall the results suggest that the local distortions accompanying the Ga incorporation are accommodated more by the La positions than the oxygen channels, thus keeping these channels open for conduction. In going to the smaller Nd, it is possible that this local distortion is no longer accommodated by the rare earth positions, but begins to significantly affect the oxygen channels, either causing an increase in the migration energy or leading to "trapping" of oxygen interstitial defects. Further modelling work on doped $\text{Nd}_{9.33}\text{Si}_6\text{O}_{26}$ is required to investigate this.

In conclusion the results show that the effect of dopants on the conductivity of apatite-type ionic conductors can be strongly influenced by the rare earth size. In the case of La silicate apatites, Ga doping leads to an enhancement of the conductivity, while for Nd silicate apatites a decrease in the conductivities at low temperatures and a significant increase in the activation energy are observed. The increase in activation energy for

the Nd containing systems may be related to a higher migration energy or "trapping" of oxygen interstitials around the Ga dopant.

4. Acknowledgements

We would like to thank EPSRC for funding.

5. References

- [1] S. Nakayama, H. Aono, Y. Sadaoka, Chem. Lett. 431 (1995).
- [2] S. Nakayama, M. Sakamoto, J. Eur. Ceram. Soc. **18**, 1413 (1998).
- [3] S. Nakayama, M. Sakamoto, M. Higuchi, K. Kodaira, M. Sato, S. Kakita, T. Suzuki, K. Itoh, J. Eur. Ceram. Soc. **19**, 507 (1999).
- [4] H. Arikawa, H. Nishiguchi, T. Ishihara, Y. Takita, Solid State Ionics **136-137**, 31 (2000).
- [5] J.E.H. Sansom, L. Hildebrandt, P.R. Slater, Ionics **8**, 155 (2002).
- [6] J.E.H. Sansom and P.R. Slater, Solid State Phenomena **90-91**, 189, (2003).
- [7] S. Nakayama and M. Sakamoto, J. Mater. Sci. Lett. **20**, 1627 (2001).
- [8] P. Berastegui, S. Hull, F.J. Garcia Garcia and J. Grins, J. Solid State Chem. **168**, 294 (2002).
- [9] P.R. Slater, J.E.H. Sansom, J.R. Tolchard, and M.S. Islam, Proc. MRS Conf. Solid State Ionics-2002, 567 (2003).
- [10] L. Leon-Reina, M.E. Martin-Sedeno, E.R. Losilla, A. Caberza, M. Martinez-Lara, S. Bruque, F.M.B. Marques, D.V. Sheptvakov, M.A.G. Aranda, Chem. Mater. **15**, 2099 (2003).
- [11] J.R. Tolchard, J.E.H. Sansom, P.R. Slater, M.S. Islam, J. Solid State Electrochem. **8**, 668 (2004).
- [12] S. Tao, J.T.S. Irvine, Mater. Res. Bull. **36**, 1245 (2001).
- [13] J.E.H. Sansom, D. Richings, P.R. Slater, Solid State Ionics **139**, 205 (2001).
- [14] E.J. Abram, D.C. Sinclair, A.R. West, J. Mater. Chem. **11**, 1978 (2001).
- [15] J. McFarlane, S. Barth, M. Swaffer, J.E.H. Sansom, P.R. Slater, Ionics **8**, 149 (2002).
- [16] M.S. Islam, J.R. Tolchard, P.R. Slater, Chem. Commun. 1486 (2003).
- [17] J.R. Tolchard, M.S. Islam, P.R. Slater, J. Mater. Chem. **13**, 1956 (2003).
- [18] J.E.H. Sansom and P.R. Slater, Proc. 5th Euro SOFC forum **2**, 627 (2002).

- [19] P.R. Slater and J.E.H. Sansom, Solid State Phenomena **90-91**, 195 (2003).
- [20] J.R. Tolchard, J.E.H. Sansom, P.R. Slater and M.S. Islam, Solid State Ionics **167**, 17 (2004).
- [21] L. Leon-Reina, E.R. Losilla, M. Martinez-Lara, S. Bruque, M.A.G. Aranda, J. Mater. Chem. **14**, 1142 (2004).
- [22] A.L. Shaula, V.V. Kharton, M.V. Patrakeevev, J.C. Waerenborgh, D.P. Rojas, N.P. Vyshatko, E.V. Tsipis, A.A. Yaremchenko, F.M.B. Marques, Mater. Res. Bull. **39**, 763 (2004).
- [23] A.A. Yaremchenko, A.L. Shaula, V.V. Kharton, J.C. Waerenborgh, D.P. Rojas, M.V. Patrakeevev, F.M.B. Marques, Solid State Ionics **171**, 51 (2004).
- [24] A. Najib, J.E.H. Sansom, J.R. Tolchard, M.S. Islam, P.R. Slater, Dalton Trans. 19,3106 (2004).
- [25] J.R. Tolchard, M.S. Islam, P.R. Slater, manuscript in preparation.
- Paper presented at the Patras Conference on Solid State Ionics - Transport Properties, Patras, Greece, Sept. 14 - 18, 2004.*
- Manuscript rec. Sept. 10, 2004; acc. Oct. 30, 2004.*